Dissociation of Toluene Cation: A New Potential Energy Surface

Joong Chul Choe*

Department of Chemistry, University of Suwon, P.O. Box 77, Suwon 440-600, Korea

Received: March 1, 2006; In Final Form: April 4, 2006

The potential energy surface (PES) for the formation of tropylium and benzylium ions from toluene cation (**1**) has been explored theoretically. Quantum chemical calculations at the B3LYP/6-311++G** and G3//B3LYP levels were performed. A pathway to form *o*-isotoluene (5-methylene-1,3-cyclohexadiene) cation (**5**) from **1** was found. The isomerization occurs by two consecutive 1,2-H shifts from CH_3 to the ortho position of the aromatic ring via a distonic benzenium cation (**2**), which is also an intermediate in the well-known isomerization of **1** to cycloheptatriene cation (**4**). Since the barrier for the formation of **2** is the highest in the two isomerization pathways, **1**, **4**, and **5** are interconvertible energetically prior to dissociation. The benzylium ion can be produced via **5** as well as from **1** and the tropylium ion via **4**. Rice−Ramsperger−Kassel−Marcus model calculations were carried out based on the obtained PES. The result agrees with previous experimental observations. From a theoretical analysis of kinetics of the isomerizations and dissociations, we suggest that **5** plays an important role in the formation of $C_7H_7^+$ from **1**.

1. Introduction

The formation of $C_7H_7^+$ from toluene molecular cation (**1**) is one of the most extensively studied reactions in the field of gas-phase ion chemistry. Since Rylander et al.[1] suggested the seven-membered-ring tropylium ion (**Tr**) for the product $C_7H_7^+$ in 1957, the kinetics and mechanism of formation of **Tr** and/or benzylium ion (**Bz**) from $C_7H_8^{+\bullet}$ [2−26] or other alkylbenzene cations[25−37] have been the focus of numerous researchers for the past half century. Various experimental techniques have been used to determine the dissociation rate constants, **Tr**/**Bz** branching ratios, kinetic energy releases, isotope effects, etc. It is well-known that **Bz** is formed by a direct cleavage from **1** and **Tr** via a rearrangement to cycloheptatriene cation (**4**). This has been confirmed by a theoretical potential energy surface (PES) obtained by Lifshitz et al.[17] According to the PES, a H atom of the methyl group migrates initially to the ipso position of the aromatic ring to form a distonic benzenium ion (**2**), and **2** undergoes further isomerizations to norcaradiene cation (**3**) and **4** (Scheme 1). The investigators showed that Rice−Ramsperger−Kassel−Marcus (RRKM)[38] model calculations based on the PES can fit well experimental **Tr**/**Bz** ratios and dissociation rate constants. These studies are excellently reviewed by Lifshitz.[20]

On the other hand, the role of *o*-isotoluene (5-methylene-1,3-cyclohexadiene) cation (**5**) in the formation of $C_7H_7^+$ from **1** has been overlooked since the report of the PES of Lifshitz et al. In earlier mass spectrometric studies, it was suggested

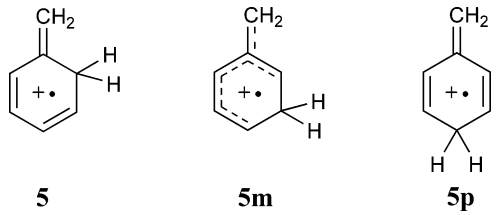

5 **5m** **5p**

that three isomers **1**, **4**, and **5** interconvert prior to dissociation.[3,4] Dewar and Landman[22] proposed **5** as a possible intermediate in the isomerization of **1** → **4** based on MINDO/3 calculations, agreeing with the experimental observations. They suggested that **5** is formed from 1,3-H shift from the methyl group to the ortho position of the aromatic ring. Lifshitz et al.,[17] however, excluded the pathway in their analysis of the dissociation kinetics because there are high barriers along the pathway. This is supported in a recent theoretical study by Grützmacher and Harting.[25] It is probable, however, that an isomerization pathway for **1** → **5**, energetically comparable and hence competitive to the pathway for **1** → **4** in Scheme 1, has not been found yet theoretically.

In this work, we have explored the theoretical PES for loss of $H^\bullet$ from **1** with attention to involvement of **5**. On the basis of the obtained PES, RRKM model calculations have been carried out to fit the previous experimental **Tr**/**Bz** ratios and dissociation rate constants. From the results, the dissociation kinetics of the formation of $C_7H_7^+$ will be discussed in detail.

2. Methods

Molecular orbital calculations were performed with the Gaussian 03 suite of programs.[39] Geometry optimizations for the stationary points were carried out at the unrestricted B3LYP level of density functional theory (DFT)[40] with the 6-311++G** basis set. Transition state (TS) geometries connecting the stationary points were searched and checked by calculating the intrinsic reaction coordinates at the same level. Unrestricted HF calculations for the $C_7H_8^{+\bullet}$ species resulted in severe spin contamination as reported by Lifshitz et al.[17] Spin contamination of the DFT calculations was satisfactory. All the expectation values for the spin operator S^2 were in the range of 0.75−0.77. The harmonic frequencies calculated at the B3LYP/6-311++G** level were used for zero point vibrational energy (ZPVE) corrections without scaling. For better accuracy of the energies, Gaussian-3 (G3) theory calculations using the B3LYP density functional method (G3//B3LYP)[41] were performed. In G3//B3LYP calculations, the geometries are obtained at the B3LYP/6-31G* level, and the ZPVEs are obtained at the same level and scaled by 0.96. All the other steps remain the same as in

* Phone: +82-31-220-2150. Fax: +82-31-222-9385. E-mail: jcchoe@suwon.ac.kr.

10.1021/jp0612782 CCC: $33.50
Published on Web 05/28/2006

SCHEME 1

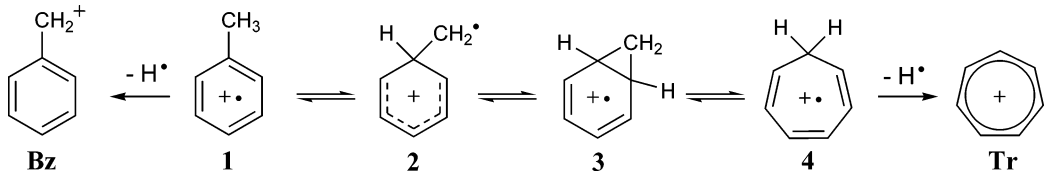

the G3 method[42] with the exception of the values of the higher level correction parameters.

The RRKM expression[38] was used to calculate the rate-energy dependences:

$$k(E) = \frac{\sigma N^{\ddagger}(E - E_0)}{h\rho(E)} \quad (1)$$

where E is the reactant internal energy, E_0 is the critical energy of the reaction, $N^{\ddagger}$ is the sum of states of the transition state, ρ is the density of states of the reactant, and σ is the reaction path degeneracy. $N^{\ddagger}$ and ρ were evaluated by direct count of states with use of the Beyer−Swinehart algorithm.[38,43]

3. Results and Discussion

All of the stationary points in Scheme 1 and the TSs connecting them except the TS (**TS1Bz**) for **1** → **Bz** + H• were optimized at the B3LYP/6-311++G** levels. Their relative energies are listed in Table 1, and the geometrical structures for the isomers and TSs are shown in Figure 1. The energy for

TABLE 1: Relative Energies and Entropies of Relevant Species

species	energy, kJ mol^{-1}				entropy,[e] J K^{-1} mol^{-1}
	B3LYP/6-311++G**[b]	G3//B3LYP	exptl[c]	G3//B3LYP(-d_8)[d]	
toluene$^{+\bullet}$ (**1**)	0	0	0	0	0
$C_6H_6CH_2^{+\bullet}$ (**2**)[a]	147	144		147	−1
norcaradiene$^{+\bullet}$ (**3**)	91	80		79	−24
cycloheptatriene$^{+\bullet}$ (**4**)	62	75	80	74	−17
o-isotoluene$^{+\bullet}$ (**5**)	30	38		38	−14
m-isotoluene$^{+\bullet}$ (**5m**)	87	95		96	−7
p-isotoluene$^{+\bullet}$ (**5p**)	40	46		46	−14
Bz + H•	224	216	218	224	
Tr + H•	188	188	164	196	
TS12	153	159		162	−21
TS23	154	149		151	−20
TS25	153	149		152	−20
TS34	125	116		115	−35
TS55m	117	116		120	−26
TS5m5p	121	119		124	−26
TS4Tr	201	207		212	−13
TS5Bz	229	223		230	−1
TS5pBz	226	219		226	3

[a] A distonic benzenium cation. See Scheme 1. [b] The ZPVE calculated is included without scaling. [c] From experimental heats of formation at 0 K in ref 44. The heat of formation of **Bz** was taken from ref 45. [d] For the $C_7D_8^{+\bullet}$ species. [e] Calculated at 1000 K from the vibrational frequencies calculated at the B3LYP/6-31G* level and scaled by 0.96. Contribution of the CH_3 internal rotation to **1** is 29 J K^{-1} mol^{-1}.

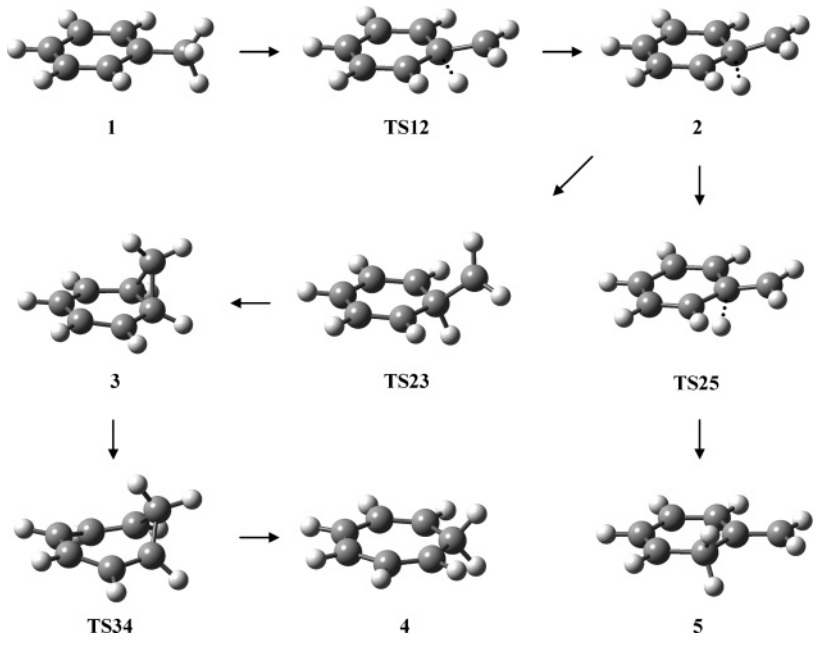

Figure 1. The isomerization pathway of **1** obtained by B3LYP/6-311++G** calculations.

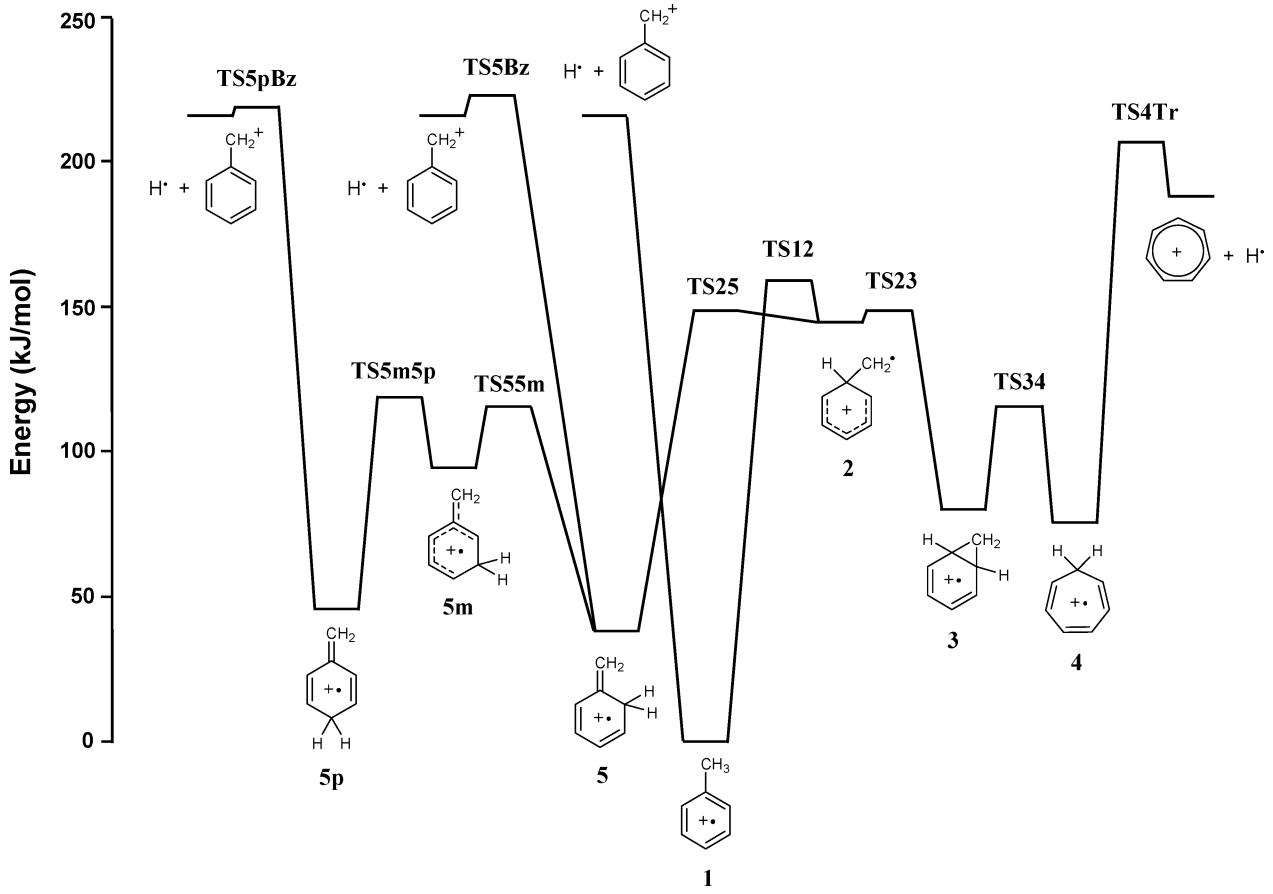

Figure 2. The potential energy surface obtained by G3//B3LYP calculations.

1 → **Bz** + H• is critical in RRKM model calculations. The calculated one is higher than the experimental one by 6 kJ mol^{-1} (Table 1). The G3//B3LYP calculations resulted in a better agreement. The discrepancy is reduced to 2 kJ mol^{-1}. The differences between the relative energies calculated by the B3LYP and G3//B3LYP methods are within ~10 kJ mol^{-1}. The PES constructed from the G3//B3LYP calculations is depicted in Figure 2. For this pathway, Lifshitz et al.[17] and Grützmacher and Harting[25] have obtained similar PESs by HF calculations. The latter investigators, however, reported that **2** was not a stable species in their DFT calculations. As shown in Figure 2, **2** is much less stable than other isomers. It rearranges to other isomers rapidly after formation.

More importantly, we found another isomerization pathway of **2**, not reported so far. The *ipso*-H atom of **2** can either retain its position or migrate to the adjacent ortho position, which forms **3** or **5**, respectively (see Figure 1). The former process is a step in the pathway to form **4** mentioned above, which can produce **Tr** eventually. The latter is a newly found pathway to form **5**, occurring by two consecutive 1,2-H shifts. The barriers (**TS23** and **TS25**) for two isomerizations are almost the same. In other words, **2** is a common intermediate for interconversion of **1**, **4**, and **5**. Analogous pathways have been suggested in our recent study[46] on the dissociation of phenylsilane cation. **5** can undergo further 1,2-H shifts to form the meta and para isomers, **5m** and **5p** ("H ring walk"). **5** and **5p**, more stable than **5m**, can produce **Bz** with small reverse barriers. This means that the dissociation kinetics would be more complicated than understood without considering **5** so far.

The PES in Figure 2 shows that interconversion of the stable $C_7H_8^{+\bullet}$ isomers can occur readily prior to dissociation. The highest barrier (**TS12**) for the interconversion lies lower than the dissociation threshold (**TS4Tr**) by 48 kJ mol^{-1}. However, an entropic factor is as important as an energetic factor in reaction kinetics. The transition state RRKM theory is adequate to predict the kinetics. We calculated the dissociation rate constants of **1** and **Tr**/**Bz** ratios by RRKM modeling based on the obtained PES to compare with the experimental data.

Since several isomers are involved in the dissociation, RRKM calculations were carried out under some approximations. First, we treat the PES as a three-well PES. Since **TS34** lies lower than **TS4Tr** or **TS23**, interconversion of **3** and **4** would be faster than dissociation to **Tr** or isomerization to **2**. Therefore, **3** and **4** can be considered as a stable species, which will be designated by **4** for convenience. Similarly, the three isotoluene isomeric ions are considered as a species, **5**. In addition, since the lifetime of **2** must be very short, each of the two-step isomerizations via **2** is approximated by a one-step isomerization by using the steady-state approximation.[47] Then, the complicated isomerizations are well approximated by a cyclic reaction (Scheme 2). The kinetic equations associated with the three-well-two-product model are given by

$$\frac{d[\mathbf{1}]}{dt} = k_2[\mathbf{4}] + k_6[\mathbf{5}] - (k_1 + k_4 + k_5)[\mathbf{1}] \quad (2)$$

$$\frac{d[\mathbf{4}]}{dt} = k_1[\mathbf{1}] + k_8[\mathbf{5}] - (k_2 + k_3 + k_9)[\mathbf{4}] \quad (3)$$

$$\frac{d[\mathbf{5}]}{dt} = k_5[\mathbf{1}] + k_9[\mathbf{4}] - (k_6 + k_7 + k_8)[\mathbf{5}] \quad (4)$$

$$\frac{d[\mathbf{Tr}]}{dt} = k_3[\mathbf{4}] \quad (5)$$

$$\frac{d[\mathbf{Bz}]}{dt} = k_4[\mathbf{1}] + k_7[\mathbf{5}] \quad (6)$$

At time $t = 0$ the initial concentrations of the three isomers are

SCHEME 2

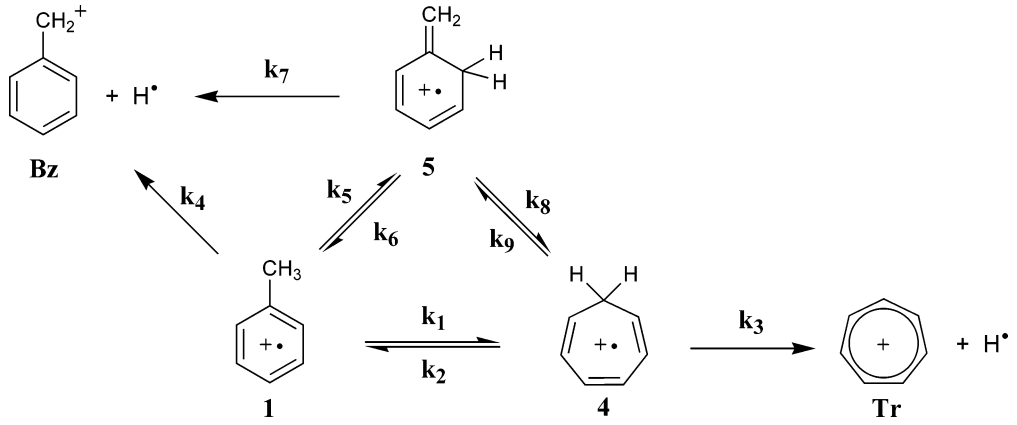

[**1**] = [**1**]$_0$ and [**4**] = [**5**] = 0. The exact solution of these differential equations is very complicated. A simplified solution can be obtained by application of the steady-state approximation. Since **4** and **5** are less stable than **1**, it is expected that their lifetimes are shorter than that of **1**, which will be proved below. Then, the following approximation is valid.

$$\frac{d[\mathbf{4}]}{dt} \approx \frac{d[\mathbf{5}]}{dt} \approx 0 \tag{7}$$

From eqs 2−4 and 7, the following simple solution is obtained:

$$[\mathbf{1}] = [\mathbf{1}]_0 \exp(-k_{obs}t) \tag{8}$$

where k_{obs} is the observable dissociation rate constant of **1** approximated by

$$k_{obs} \approx k_1 + k_4 + k_5 - k_2\alpha - k_6\beta \tag{9}$$

where $\alpha = (k_5k_8 + k_1\gamma)/(\gamma\delta - k_8k_9)$, $\beta = (k_1k_9 + k_5\delta)/(\gamma\delta - k_8k_9)$, $\gamma = k_6 + k_7 + k_8$, and $\delta = k_2 + k_3 + k_9$. From eqs 3−7, the **Tr**/**Bz** ratio is approximated by

$$\frac{[\mathbf{Tr}]}{[\mathbf{Bz}]} \approx \frac{k_3\alpha}{k_4 + k_7\beta} \tag{10}$$

Under the above approximation, the dissociation rate constant (k_{obs}) and **Tr**/**Bz** ratio are described by means of the nine rate constants, k_1-k_9. The individual RRKM rate-energy dependences were calculated. The G3//B3LYP energies were used for the critical energies. The vibrational frequencies calculated at the B3LYP/6-31G* level with the geometries optimized at the same level were used with scaling by 0.96[48] in the absence of recommended scaling factors for other basis sets of the B3LYP method. Both state densities of **3** and **4** were considered in the calculations of k_2, k_3, and k_9. For k_6, k_7, and k_8, all state densities of **5**, **5m**, and **5p** and both state sums of **TS5Bz** and **TS5pBz** were considered. Since it is known that the CH_3 rotation is nearly free in **1**,[49] the CH_3 torsional mode was replaced by the internal rotation in the calculation of density of states of **1**. **TS1Bz** presents a problem in the RRKM calculations because no saddle point was found in the dissociation of **1** to **Bz** + H•. Therefore, the distance between the C and H atoms of the methyl group of **1** was increased with optimization of all other coordinates (see Figure 3). The best geometry for this loose TS will be chosen by comparing the resultant k_{obs} values and **Tr**/**Bz** ratios with experimental ones.

Two research groups reported experimental dissociation rate constants of **1**. Bombach et al.[8] measured the rate constants using photoelectron−photoion coincidence (PEPICO) spectroscopy on a microsecond time scale. They interpreted that the $k(E)$ curves for the formation of **Tr** and **Bz** cross each other, which has been ruled out by subsequent studies.[7,13,20] In addition, their measured rates are much faster than those investigated later.[13,18] The well-accepted rate constants were measured in a time-resolved photodissociation study by Huang and Dunbar,[13] which will be used here for comparison. Reliable **Tr**/**Bz** ratios were obtained by using photodissociation[11] and charge exchange mass spectrometry[14] as a function of the energy.

All the individual rate constants except k_4 were calculated as described above without any further adjustment. To calculate k_4 reasonably, vibrational frequencies for the optimized geometries at separating C−H distances of 1.6−3.0 Å (at 0.2 Å intervals along the coordinate in Figure 3) were calculated and used for **TS1Bz**. From k_1-k_9 thus calculated, k_{obs} and the **Tr**/**Bz** ratio were evaluated and compared with experimental values. The best fit was obtained with **TS1Bz** at the C−H distance of 2.0 Å (Model I, see Table 2). The resultant individual rate constants are shown in Figure 4. The agreement between the RRKM calculations and experiments is not excellent as shown in Figures 5 and 6. It is to be noted that the energetic data and vibrational frequencies for a total of 13 stationary points[50] obtained by quantum chemical calculations were used in the calculations under the approximations mentioned above. Considering this, the agreement achieved here is remarkable even though cancellation by possible positive and negative errors arising from the individual steps cannot be ruled out. The

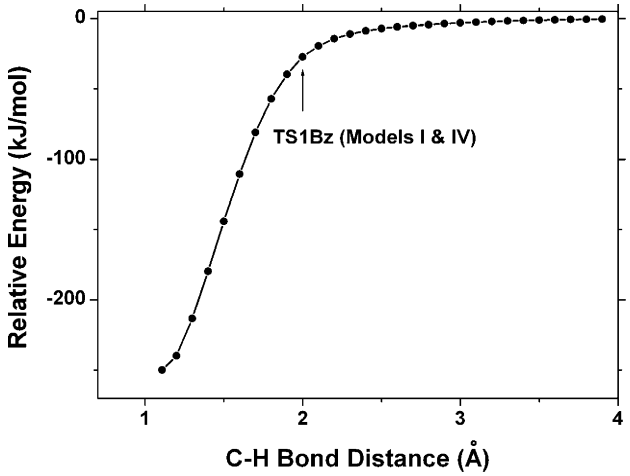

Figure 3. Dissociation path energy calculations for **Bz**-H as a function of the separating C−H distance (the B3LYP/6-31G* result). The best RRKM fitting was obtained with **TS1Bz** at the C−H distance of 2.0 Å, indicated by the arrow.

TABLE 2: Summary of RRKM Modeling

model	scaling factor for vibrational frequencies[a] reactant	TS	C−H distance of **TS1Bz** (Å)
I	0.96	0.96	2.0
II	0.96	0.96	2.6
III	0.96	0.96	1.6
IV	0.96	1.02	2.0

[a] Vibrational frequencies were calculated at the B3LYP/6-31G* level. The scaling factor recommended in ref 48 is 0.96.

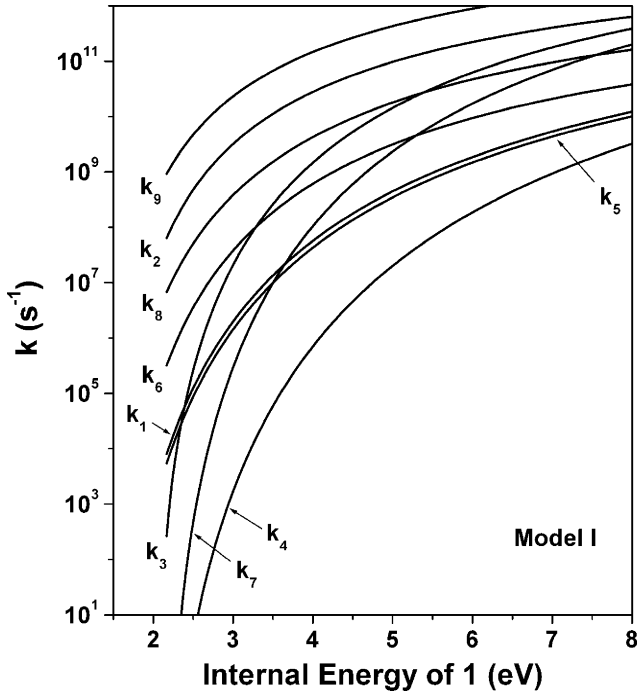

Figure 4. RRKM rate-energy dependences for k_1-k_9 calculated by Model I.

calculated k_{obs} is rather insensitive to the C−H distance assumed for **TS1Bz** at low energies where experimental data are available, while those with different C−H distances diverge as energy increases (see Figure 5). Since the **Tr**/**Bz** ratio was measured over a wider energy range (2.4−7.0 eV), it is more useful in comparison. The calculated abundance of **Tr** is sensitive to the C−H distance of **TS1Bz** as shown in Figure 6. At low energies the TS at the C−H distance 2.6 Å (Model II) shows a better agreement. As the distance decreases, the abundance of **Tr** increases. At the distance of 2.0 Å, the agreement between calculated and experimental abundance ratios is the best. Decreasing the distance less than 2.0 Å hardly affects k_{obs} or **Tr**/**Bz** ratios (see Figures 5 and 6). The distances far less than 2.0 Å, however, are too short as structures for **TS1Bz** considering the energy calculations shown in Figure 3.

For unimolecular reactions without reverse barriers, modified RRKM theories such as the variational transition state theory (VTST) and the statistical adiabatic channel model (SACM) are more appropriate for modeling of loose transition states than the normal RRKM theory employed here. We have not attempted to estimate k_4 by such modified RRKM theories since k_4 is one of the nine rate constants determining k_{obs} with limited accuracy of theoretical molecular parameters and energetic data for estimation of the other rate constants. The present estimation of k_4 by the normal RRKM calculations is adequate for the purpose of understanding the dissociation kinetics of the $C_7H_8^{+\bullet}$ isomers qualitatively. Instead we will mention some recent

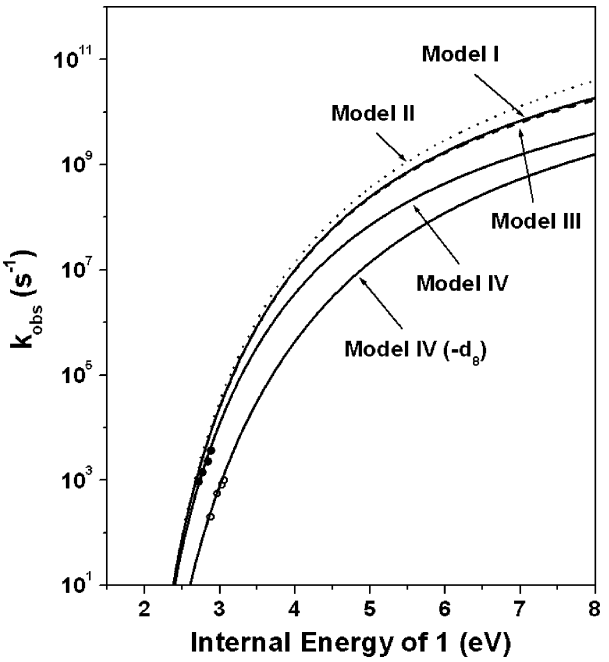

Figure 5. Rate-energy dependences for k_{obs}. Closed and open circles are experimental results of photodissociation of toluene and toluene-d_8 cations, respectively.[13] Curves are the result of RRKM model calculations.

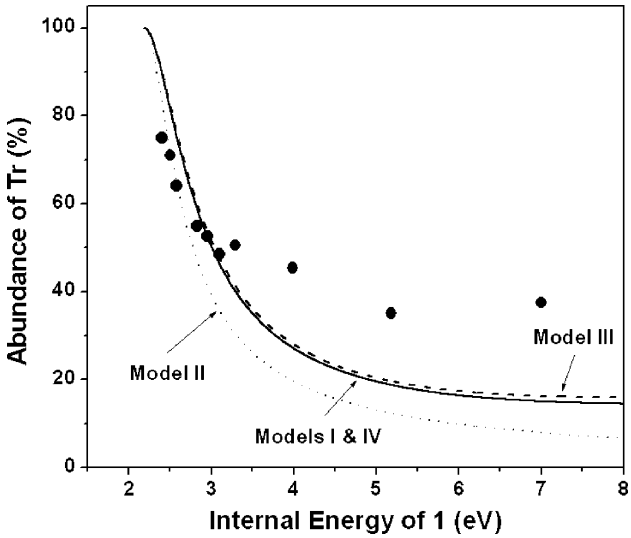

Figure 6. The relative abundance of **Tr**, [**Tr**]/([**Tr**] + [**Bz**]). Circles are the results of photodissociation[11] and charge exchange[14] experiments corrected for thermal energies by Lifshitz et al.[17] Curves are the results of RRKM model calculations.

results of VTST or SACM calculations. For the H$^\bullet$ loss from benzene cation, Klippenstein et al.[51] and Troe et al.[36] carried out the VTST and SACM/CT (classical trajectory) calculations for $k(E)$, respectively. The two results are nearly the same and agree well with the normal RRKM result at rate constants larger than 10^4 s^{-1}. Near the reaction threshold, they predict somewhat lower rate constants than the normal RRKM result, which resulted in higher critical energies. The SACM/CT $k(E)$ calculations[36] for the formation of $C_7H_7^+$ from *n*-butylbenzene cation gave a similar result in comparison with the normal RRKM calculation. The two model calculations agree well at rate constants larger than 10^3 s^{-1}.

Decreasing the C−H distance of **TS1Bz** makes the TS tighter and results in a decrease of k_4. Then, contribution of the route **1** → **Bz** + H$^\bullet$ to the formation of **Bz** would decrease, since **Bz**

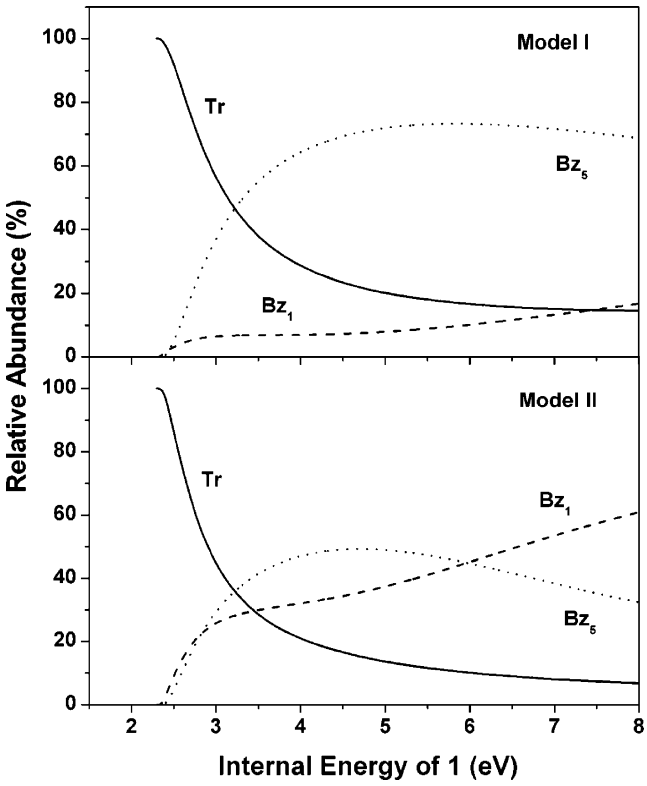

Figure 7. Relative abundances of **Tr**, $\mathbf{Bz_1}$, and $\mathbf{Bz_5}$ calculated by RRKM Models I and II. $\mathbf{Bz_1}$ and $\mathbf{Bz_5}$ denote **Bz** formed from **1** and via **5**, respectively.

can be produced via **5** as well as from **1**. The denominator of eq 10 is the sum of the two contributions. The abundance ratio of **Bz** formed from **1** and via **5**, $[\mathbf{Bz}]_1$:$[\mathbf{Bz}]_5$, is k_4:$k_7\beta$. The calculated result is shown Figure 7 as a function of the energy together with the relative abundance of **Tr**. At the C−H distance of 2.0 Å (Model I) $[\mathbf{Bz}]_1$ is around 10% of the total product ions, less than $[\mathbf{Bz}]_5$. Since $[\mathbf{Bz}]_1$ would become far less than $[\mathbf{Bz}]_5$ at C−H distances less than 2.0 Å, the contribution of $\mathbf{1} \rightarrow \mathbf{Bz} + H^{\bullet}$ to the **Tr**/**Bz** ratio or k_{obs} becomes negligible compared to that of formation of **Bz** via **5**. It is to be noted that the latter contribution, ignored in the previous theoretical study,[17] is considerable. Even at the C−H distance of 2.6 Å (Model II) $[\mathbf{Bz}]_5$ is similar to or larger than $[\mathbf{Bz}]_1$ up to ∼6 eV (see Figure 7). This clearly shows that contribution of isotoluene cations to the formation of $C_7H_7^+$ from **1** should not be ignored.

From the rate-energy dependences in Figure 4, the kinetics of isomerizations and dissociations of the various $C_7H_8^{+\bullet}$ ions can be predicted. Starting from **1**, the isomerizations to **4** and **5** are much faster than the dissociation to **Bz** at low energies (k_1, $k_5 \gg k_4$). As energy increases the dissociation rate constant, k_4, increases more rapidly and would become larger than the isomerizations at higher energies. The result of $k_1 \approx k_5$ indicates that initially **4** and **5** are formed with similar abundances. Since k_9 is much larger than k_8, however, the abundance of **5** would be much larger after interconversion with **4**. Then, the abundance of **4** becomes very small. In addition, most of **5** ions return to **1** (mainly at low energies, $k_6 > k_5$, k_7) or dissociate to **Bz** (mainly at high energies, $k_7 > k_5$, k_6) faster than its formation from **1**. This means that **4** and **5** are more reactive than **1** and have little time to accumulate, and the steady-state approximation (eq 7) applied above is valid. One of the reasons why **1** is less reactive is due to the free internal rotation of the methyl group. Evaluation of relative entropies of the relevant species is helpful in understanding the kinetics of isomerizations and dissociations. The relative entropy between stable species can be considered as the reaction entropy, and that between a reactant and a TS as the activation entropy ($\Delta S^{\ddagger}$). The relative entropies evaluated at 1000 K by using the vibrational frequencies calculated and scaled by 0.96 and the rotational constant (5.5 cm^{-1}) for the internal rotation of **1** are listed in Table 1. All the stable species have negative entropies relative to **1**. The higher the entropy is, the more stable the species is without considering the energetic factor, because the density of states increases with the entropy. In other words, the isomers such as **3**, **4**, **5**, **5m**, and **5p** are less stable than **1** entropically as well as energetically. Contribution of the internal rotation to the entropy of **1** is evaluated as 29 J K^{-1} mol^{-1}, which is the main reason for the particular entropic stability of **1**. Since **5** and **5p** are energetically and entropically more stable than **3** and **4**, the abundances of the stable isomers at preequilibrium prior to dissociation would be on the order of **1** > **5**, **5p** > **3**, **4**. This agrees with the above prediction from the rate-energy dependences.

Starting from **4**, it rapidly isomerizes to **5** or **1** prior to dissociation to **Tr** (k_9, $k_2 > k_3$). As energy increases, the dissociation rate increases more rapidly than the isomerizations. The kinetics of isomerizations and dissociation starting from **5** is similar to those of **1** and **4**. At low energies its isomerizations are faster than dissociation to **Bz**, and at high energies the reverse is true. Figure 4 shows that the slopes (k_3, k_4, and k_7) for dissociations are larger than those for isomerizations. This means that the stable $C_7H_8^+$ isomers rapidly interconvert prior to dissociation at low energies, and the dissociations can occur faster than the interconversion at high energies. This prediction agrees with the previous experimental observations. In early work, McLafferty and co-workers[2−4] carried out mass spectrometric investigations on several $C_7H_8^{+\bullet}$ isomers with deuterium labeling. They compared dissociations of deuterium-labeled ions of **1**, **4**, and **5** (**5** was generated from 2-phenylethanol) by determining isotope effects and degrees of H-scrambling.[3] It was concluded that for their metastable dissociations, occurring on a microsecond time scale, **1**, **4**, and **5** isomerize to a common structure prior to dissociation, and **5** ions of higher energies undergo direct cleavage loss of $H^{\bullet}$ prior to isomerization. In a later study,[4] isomerization of **1** to **5** was suggested. Subsequent studies by several investigators showed the distinct behavior of **5** generated from *n*-butylbenzene or 2-phenylethanol, using techniques of photodissociation[12] and collision-induced dissociation.[6] This indicates the stability of **5** and its distinguishable dissociation at high energies as predicted above. Bartmess[15] and Bally et al.[16] generated **5** and/or **5p** from their neutrals and confirmed their distinct entity on the $C_7H_8^{+\bullet}$ hypersurface.

The experimental observation of **Tr** at high energies can be due to further isomerization of **Bz** after formation. Very recently, Fridgen et al.[35] reported that **Bz** formed from ethylbenzene cation can undergo isomerization to **Tr**. From a theoretical analysis of experimental data, they suggested that the threshold for the isomerization is ∼4.5 eV of the internal energy of ethylbenzene cation. Comparing the threshold (∼160 kJ mol^{-1}) calculated for the formation of **Bz** from ethylbenzene cation with that (∼220 kJ mol^{-1}) from **1**, it is possible that the **1** ions of energies higher than ∼5.1 eV can undergo $\mathbf{1} \rightarrow \mathbf{Bz}$ (+ $H^{\bullet}$) → **Tr**. This suggests that the isomerization $\mathbf{Bz} \rightarrow \mathbf{Tr}$ would make a contribution to the experimental abundance of **Tr** at 7.0 eV in Figure 6.

An attempt was made to improve the rate calculations by adjusting parameters used in RRKM modeling, even though the above analysis is enough to understand the kinetics qualitatively.

The k_{obs} values calculated overestimate the experimental ones by a factor of ~2. The rate constant is lowered by increasing the critical energy and/or vibrational frequencies of the TS (i.e., tighter TS) in RRKM calculations. The accuracy of TS frequencies and energies obtained by quantum chemical calculations has not been evaluated. We varied vibrational frequencies of the TSs without changing the critical energies since the activation entropies evaluated from the vibrational frequencies scaled by 0.96 indicate somewhat looser TSs. For example, the $\Delta S_{1000K}^{\ddagger}$ values for **4** → **Tr** + H• and **5** → **Bz** + H•, occurring via tight TSs, are positive values (4 and 13 J K^{-1} mol^{-1}, respectively, evaluated from the data listed in Table 1), even though generally $\Delta S^{\ddagger}$ is a negative value for the reaction occurring via a tight TS.[38] Use of a global scaling factor of 1.02 (Model IV, see Table 2) for vibrational frequencies of TSs resulted in the best agreement between calculated and experimental k_{obs} values (see Figure 5). It is usual that the scaling factor ($F^{\ddagger}$) for TS frequencies required for RRKM fitting is larger than that (F) for reactant frequencies as in this case. For the formation of **Tr** from ethylbenzene cation, Fridgen et al.[35] reported that $F = 0.9$ and $F^{\ddagger} = 1.09$. Muntean and Armentrout[37] used $F = 0.9804$ and $F^{\ddagger} = 1.039$ for the best RRKM $k(E)$ fit for the formation of $C_7H_8^{+\bullet}$ from *n*-butylbenzene cation. The Tr/Bz ratio curve calculated by model IV was essentially the same as that of Model I. The lack of experimental k_{obs} data at high energies limits the accuracy of the theoretical prediction of $k_{obs}(E)$. We do not insist that this improvement is the best with high confidence because of limited accuracy of the present theoretical estimation for a lot of energies and vibrational frequencies involved in isomerization and dissociation steps. This improved model can be used for prediction of the intermolecular isotope effect. Huang and Dunbar[13] measured the rate constants for the photodissociation of perdeuterated toluene cation as well. The relative energies and vibrational frequencies of the $C_7D_8^{+\bullet}$ species were calculated. The G3//B3LYP energetic data are listed in Table 1. The k_{obs} values for the dissociation of toluene-d_8 cation calculated by Model IV agree well with the experimental ones as shown in Figure 5. The lowering of the rate constants by deuteration is mainly due to higher critical energies for the isomerization and dissociation steps of the $C_7D_8^{+\bullet}$ isomers. The deuteration hardly affects the relative entropies.

4. Conclusions

A new PES for the formation of $C_7H_7^+$ from **1** was obtained by the B3LYP/6-311++G** and G3//B3LYP calculations. We found the pathway to form **5** by two consecutive 1,2-H shifts from **1**. Its energy barrier is the same as the barrier for the well-known pathway to form **4**. The distonic benzenium cation, **2**, is a common intermediate for the interconversion of **1**, **4**, and **5**. From RRKM model calculations based on the obtained PES, the dissociation rate constants and **Tr**/**Bz** ratios were obtained as a function of the energy, which agree with the previous experimental data. The calculated result predicts that the stable $C_7H_8^{+\bullet}$ isomers interconvert rapidly prior to dissociation at low energies, while they dissociate faster than the interconversion at high energies, in accordance with the experimental observations. From the kinetic analysis, we suggest that isotoluene cations make a significant contribution to the formation of **Bz** from **1**. This demands further investigations for the role of substituted isotoluene cations in dissociations of other alkylbenzene cations.

Acknowledgment. This work was supported by a Korea Research Foundation Grant funded by the Korean Government (MOEHRD) (KRF-2005-041-C00224), in which main calculations were performed using the supercomputing resource of the Korea Institute of Science and Technology Information (KISTI).

Supporting Information Available: Cartesian coordinates optimized at the B3LYP/6-311++G** level, vibrational frequencies for $C_7H_8^{+\bullet}$ and $C_7D_8^{+\bullet}$ ions calculated at the B3LYP/6-31G* level, reaction path degeneracies assumed in RRKM calculations, and RRKM rate expressions for k_1-k_9. This material is available free of charge via the Internet at http://pubs.acs.org.

References and Notes

(1) Rylander, P. N.; Meyerson, S.; Grubb, H. M. *J. Chem. Phys.* **1957**, *79*, 842.
(2) Howe, I.; McLafferty, F. W. *J. Am. Chem. Soc.* **1971**, *93*, 99.
(3) Levsen, K.; McLafferty, F. W.; Jerina, D. M. *J. Am. Chem. Soc.* **1973**, *95*, 6332.
(4) Baldwin, M. A.; McLafferty, F. W.; Jerina, D. M. *J. Am. Chem. Soc.* **1975**, *97*, 6169.
(5) McLoughlin, R. G.; Morrison, J. D.; Traeger, J. C. *Org. Mass Spectrom.* **1978**, *13*, 483.
(6) Burgers, P. C.; Terlouw, J. K.; Levsen, K. *Org. Mass Spectrom.* **1982**, *17*, 295.
(7) Buschek, J. M.; Ridal, J. J.; Holmes, J. L. *Org. Mass Spectrom.* **1988**, *23*, 543.
(8) Bombach, R.; Dannacher, J.; Stadelmann, J.-P. *J. Am. Chem. Soc.* **1983**, *105*, 4205.
(9) Dunbar, R. C. *J. Am. Chem. Soc.* **1973**, *95*, 472.
(10) Shen, J. S.; Dunbar, R. C.; Olah, G. A. *J. Am. Chem. Soc.* **1974**, *96*, 6227.
(11) Dunbar, R. C. *J. Am. Chem. Soc.* **1975**, *97*, 1382.
(12) Dunbar, R. C.; Klein, R. *J. Am. Chem. Soc.* **1977**, *99*, 11.
(13) Huang, F.-S.; Dunbar, R. C. *Int. J. Mass Spectrom. Ion Processes* **1991**, *109*, 151.
(14) Ausloos, P. *J. Am. Chem. Soc.* **1982**, *104*, 5259.
(15) Bartmess, J. E. *J. Am. Chem. Soc.* **1982**, *104*, 335.
(16) Bally, T.; Hasselmann, D.; Loosen, K. *Helv. Chim. Acta* **1985**, *68*, 345.
(17) Lifshitz, C.; Gotkis, Y.; Ioffe, A.; Laskin, J.; Shaik, S. *Int. J. Mass Spectrom. Ion Processes* **1993**, *125*, R7.
(18) Ohmichi, N.; Gotkis, I.; Steens, L.; Lifshitz, C. *Org. Mass Spectrom.* **1992**, *27*, 383.
(19) Lifshitz, C.; Gotkis, Y.; Laskin, J.; Ioffe, A.; Shaik, S. *J. Phys. Chem.* **1993**, *97*, 12291.
(20) Lifshitz, C. *Acc. Chem. Res.* **1994**, *27*, 138.
(21) Bensimon, M.; Gäumann, T.; Zhao, G. *Int. J. Mass Spectrom. Ion Processes* **1990**, *100*, 595.
(22) Dewar, M. J. S.; Landman, D. *J. Am. Chem. Soc.* **1977**, *99*, 2446.
(23) Moon, J. H.; Choe, J. C.; Kim, M. S. *J. Phys. Chem. A* **2000**, *104*, 458.
(24) Fati, D.; Lorquet, A. J.; Locht, R.; Lorquet, J. C.; Leyh, B. *J. Phys. Chem. A* **2004**, *108*, 9777.
(25) Grützmacher, H.-F.; Harting, N. *Eur. J. Mass Spectrom.* **2003**, *9*, 327.
(26) Kuck, D. *Mass Spectrom. Rev.* **1990**, *9*, 187.
(27) Kuck, D.; Grützmacher, H.-F. *Org. Mass Spectrom.* **1978**, *13*, 90.
(28) Grotemeyer, J.; Grützmacher, H.-F. In *Current Topics in Mass Spectrometry and Chemical Kinetics*; Macoll, A., Ed.; Heyden: London, UK, 1982; p 29.
(29) Harting, N.; Grützmacher, H.-F. *J. Mass Spectrom.* **1999**, *34*, 408.
(30) Baer, T.; Dutuit, O.; Mestdagh, H.; Rolando, C. *J. Phys. Chem.* **1988**, *92*, 5674.
(31) Hwang, W. G.; Moon, J. H.; Choe, J. C.; Kim, M. S. *J. Phys. Chem. A* **1998**, *102*, 7512.
(32) Oh, S. T.; Choe, J. C.; Kim, M. S. *J. Phys. Chem.* **1996**, *100*, 13367.
(33) Kim. Y. H.; Choe, J. C.; Kim, M. S. *J. Phys. Chem. A* **2001**, *105*, 5751.
(34) Fernandez, A. I.; Viggiano, A. A.; Miller, T. M.; Williams, S.; Dotan, I.; Seeley, J. V.; Troe, J. *J. Phys. Chem. A* **2004**, *108*, 9652.
(35) Fridgen, T. D.; Troe, J.; Viggiano, A. A.; Midey, A. J.; Williams, S.; McMahon, T. B. *J. Phys. Chem. A* **2004**, *108*, 5600.
(36) Troe, J.; Ushakov, V. G.; Viggiano, A. A. *J. Phys. Chem. A* **2006**, *110*, 1491.
(37) Muntean, F.; Armentrout, P. B. *J. Phys. Chem. A* **2003**, *107*, 7413.
(38) Baer, T.; Hase, W. L. *Unimolecular Reaction Dynamics*: *Theory and Experiments*; Oxford University Press: New York, 1996.
(39) Frisch, M. J.; Trucks, G. W.; Schlegel, H. B.; Scuseria, G. E.; Robb, M. A.; Cheeseman, J. R.; Montgomery, J. A., Jr.; Vreven, T.; Kudin, K.

N.; Burant, J. C.; Millam, J. M.; Iyengar, S. S.; Tomasi, J.; Barone, V.; Mennucci, B.; Cossi, M.; Scalmani, G.; Rega, N.; Petersson, G. A.; Nakatsuji, H.; Hada, M.; Ehara, M.; Toyota, K.; Fukuda, R.; Hasegawa, J.; Ishida, M.; Nakajima, T.; Honda, Y.; Kitao, O.; Nakai, H.; Klene, M.; Li, X.; Knox, J. E.; Hratchian, H. P.; Cross, J. B.; Bakken, V.; Adamo, C.; Jaramillo, J.; Gomperts, R.; Stratmann, R. E.; Yazyev, O.; Austin, A. J.; Cammi, R.; Pomelli, C.; Ochterski, J. W.; Ayala, P. Y.; Morokuma, K.; Voth, G. A.; Salvador, P.; Dannenberg, J. J.; Zakrzewski, V. G.; Dapprich, S.; Daniels, A. D.; Strain, M. C.; Farkas, O.; Malick, D. K.; Rabuck, A. D.; Raghavachari, K.; Foresman, J. B.; Ortiz, J. V.; Cui, Q.; Baboul, A. G.; Clifford, S.; Cioslowski, J.; Stefanov, B. B.; Liu, G.; Liashenko, A.; Piskorz, P.; Komaromi, I.; Martin, R. L.; Fox, D. J.; Keith, T.; Al-Laham, M. A.; Peng, C. Y.; Nanayakkara, A.; Challacombe, M.; Gill, P. M. W.; Johnson, B.; Chen, W.; Wong, M. W.; Gonzalez, C.; Pople, J. A. *Gaussian 03*, revision B.04; Gaussian, Inc.: Pittsburgh, PA, 2003.

(40) Becke, A. D. *J. Chem. Phys.* **1993**, *98*, 5648.

(41) Baboul, A. G.; Curtiss, L. A.; Redfern, P. C. *J. Chem. Phys.* **1999**, *110*, 7650.

(42) Curtiss, L. A.; Raghavachari, K.; Redfern, P. C.; Rassolov, V.; Pople, J. A. *J. Chem. Phys*. **1998**, *109*, 7764.

(43) Beyer, T.; Swinehart, D. R. *ACM Commun.* **1973**, *16*, 379.

(44) Lias, S. G.; Bartmess, J. E.; Liebman, J. F.; Holmes, J. L.; Levin, R. D.; Millard, W. G. *J. Phys. Chem. Ref. Data* **1988**, 17 (Suppl 1).

(45) Ellison, G. B.; Davico, G. E.; Bierbaum, V. M.; DePuy, C. H. *Int. J. Mass Spectrom. Ion Processes* **1996**, *156*, 109.

(46) Choe, J. C. *Int. J. Mass Spectrom*. **2004**, *237*, 1.

(47) Steinfeld, J. I.; Francisco, J. S.; Hase, W. L. *Chemical Kinetics and Dynamics*; Prentice Hall: Upper Saddle River, NJ, 1989; p 38.

(48) Scott, A. P.; Radom, L. *J. Phys. Chem*. **1996**, *100*, 16502.

(49) Lu, K.-T.; Elden, G. C.; Weisshaar, J. C. *J. Phys. Chem*. **1992**, *96*, 9742.

(50) The 13 stationary points are **1**, **3**, **4**, **5**, **5m**, **5p**, **TS12**, **TS23**, **TS25**, **TS4Tr**, **TS5Bz**, **TS5pBz**, and **TS1Bz**. The RRKM rate expressions used in the calculations of k_1-k_9 are listed in the Supporting Information.

(51) Klippenstein, S. J.; Faulk, J. D.; Dunbar, R. C. *J. Chem. Phys.* **1993**, *98*, 243.